Physics of the Earth and Planetary Interiors, 64 (1990) 1–20
Elsevier Science Publishers B.V., Amsterdam

Evidence for and implications of self-healing pulses of slip in earthquake rupture

Thomas H. Heaton

U.S. Geological Survey, 525 S. Wilson Ave, Pasadena, CA 91106 (U.S.A.)

(Received April 27, 1990; revision accepted May 23, 1990)

ABSTRACT

Heaton, T.H., 1990. Evidence for and implications of self-healing pulses of slip in earthquake rupture. Phys. Earth Planet. Inter., 64: 1–20.

Dislocation time histories of models derived from waveforms of seven earthquakes are discussed. In each model, dislocation rise times (the duration of slip for a given point on the fault) are found to be short compared to the overall duration of the earthquake (~ 10%). However, in many crack-like numerical models of dynamic rupture, the slip duration at a given point is comparable to the overall duration of the rupture; i.e. slip at a given point continues until information is received that the rupture has stopped propagating. Alternative explanations for the discrepancy between the short slip durations used to model waveforms and the long slip durations inferred from dynamic crack models are: (1) the dislocation models are unable to resolve the relatively slow parts of earthquake slip and have seriously underestimated the dislocations for these earthquakes; (2) earthquakes are composed of a sequence of small-dimension (short duration) events that are separated by locked regions (barriers); (3) rupture occurs in a narrow self-healing pulse of slip that travels along the fault surface. Evidence is discussed that suggests that slip durations are indeed short and that the self-healing slip-pulse model is the most appropriate explanation.

A qualitative model is presented that produces self-healing slip pulses. The key feature of the model is the assumption that friction on the fault surface is inversely related to the local slip velocity. The model has the following features: high static strength of materials (kilobar range), low static stress drops (in the range of tens of bars), and relatively low frictional stress during slip (less than several hundreds of bars). It is suggested that the reason that the average dislocation scales with fault length is because large-amplitude slip pulses are difficult to stop and hence tend to propagate large distances. This model may explain why seismicity and ambient stress are low along fault segments that have experienced large earthquakes. It also qualitatively explains why the recurrence time for large earthquakes may be irregular.

1. Introduction

In this paper the implications of models of the distribution of slip in time and space that have been deduced from ground motion data from seven earthquakes are discussed. Several aspects of these slip models are inconsistent with standard earthquake rupture models, and direct inspection of the slip models deduced from seismic data leads to surprising conclusions about the nature of rupture dynamics. The central issue is the duration of slip (at a given point) relative to the time required to rupture the entire fault surface. Evidence is presented that the slip duration at a given point is significantly shorter than the time to receive information about the overall rupture dimensions. Possible mechanisms to explain this observation are discussed. A qualitative rupture model is suggested that will cause the fault to heal itself shortly after the passage of the rupture front. The suggested healing mechanism is a dynamic fault friction that decreases with increasing slip velocity.

The implications of this rupture model for a variety of issues related to stress and stress changes associated with earthquakes are then discussed.

One of the most important observations of earthquake size is that

$$M_0 \propto S^{3/2} \tag{1}$$

where $\propto$ signifies proportionality, M_0 is the seismic moment, and S is the rupture area (Kanamori and Anderson, 1975). Since

$$M_0 = \mu S \overline{D} \tag{2}$$

where $\overline{D}$ is the dislocation averaged over S, this implies that

$$\overline{D} \propto \sqrt{S} \tag{3}$$

If the average stress drop $\overline{\Delta\sigma}$ of an earthquake rupture is assumed to be proportional to the average dislocation divided by a length dimension of the rupture, then

$$\overline{\Delta\sigma} \propto \mu \frac{\overline{D}}{\sqrt{S}} \tag{4}$$

Relations (3) and (4) imply that average stress drop is independent of S and therefore of M_0. A common interpretation of these scaling relations is that the average fault slip $\overline{D}$ is determined by a rupture dimension and the average stress drop, i.e. as a rupture grows over a fault surface, the final fault slip at any given point is not known until information reaches that point about the final dimensions of the rupture surface. In most dynamic rupture models, the slip duration varies from point to point on the fault and the slip time history can itself be fairly complex. However, examinination of slip histories for dynamic rupture models for faults with aspect ratios of < 2 (Day, 1982) yields a rough estimate of the average slip duration that is given by

$$T_s \approx \frac{2\sqrt{S}}{3V_r}, \tag{5}$$

where T_s is the average slip duration, V_r is the velocity of the rupture front, and $\approx$ signifies a very approximate equality. However, as I will show, this estimate of the slip duration for a point on the fault is an order of magnitude larger than that inferred from the modeling of earthquake ground motions. An alternative earthquake scaling model is presented in which the dynamic features of the propagating rupture are of central importance.

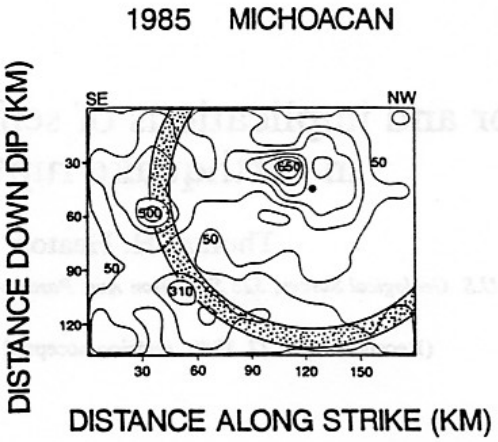

Fig. 1. Slip distribution (cm) for the $M = 8.1$ 1985 Michoacan, Mexico, earthquake derived by Mendoza and Hartzell (1989) from the simultaneous inversion of teleseismic and strong motion waveform data. The large dot denotes the hypocenter and the stippled region denotes the approximate region that is slipping at a particular instant in time.

2. Dislocation rise times

Figures 1–7 show contour maps of the slip distribution for the preferred models for the earthquakes used in this study. These models were

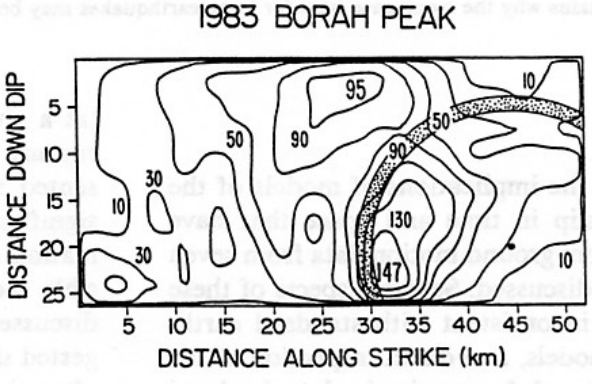

Fig. 2. Slip distribution (cm) for the $M = 7.3$ 1983 Borah Peak, ID, earthquake derived by Mendoza and Hartzell (1988) from the inversion of long- and short-period teleseismic waveform data. The large dot denotes the hypocenter stippled region denotes the approximate region that is slipping at a particular instant in time.

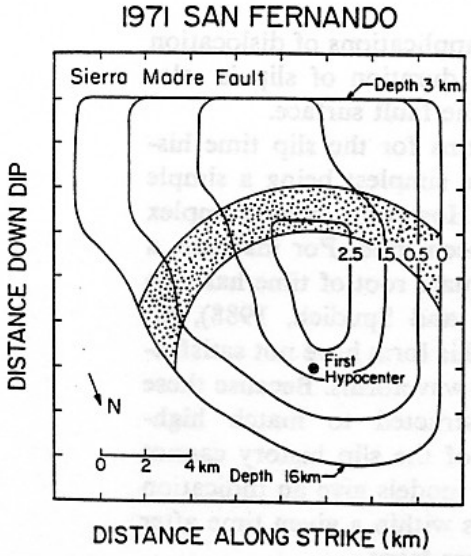

Fig. 3. Slip distribution (m) for the $M = 6.5$ 1971 San Fernando, CA, earthquake derived by Heaton (1982) from the modeling of strong motion and teleseismic waveforms and geodetic data. The earthquake was modeled as a double event and only the first event is used in this study. The stippled region denotes the approximate region that is slipping at a particular instant in time.

derived from deterministic modeling of observed strong motion and teleseismic waveforms. Although different procedures were used to produce these models, a general assumption is that rupture proceeds along the fault with an approximately constant rupture velocity and that the slip occurs in some time period (the dislocation rise time)

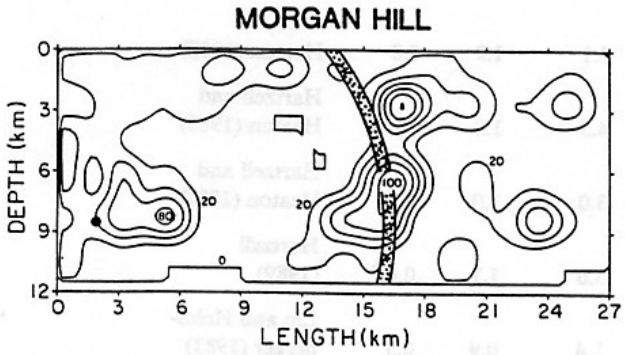

Fig. 4. Slip distribution (cm) for the $M = 6.5$ 1979 Imperial Valley, CA, earthquake derived by Hartzell and Heaton (1983) from the simultaneous inversion of strong motion and teleseismic waveform data. The large dot denotes the hypocenter and the stippled region denotes the approximate region that is slipping at a particular instant in time.

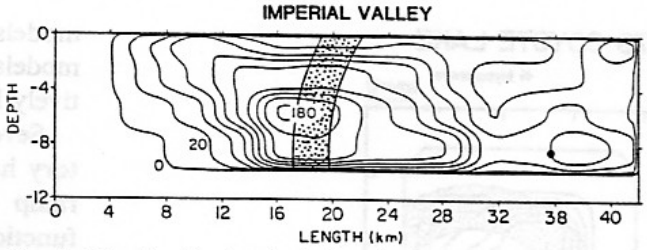

Fig. 5. Slip distribution (cm) for the $M = 6.2$ 1984 Morgan Hill, CA, earthquake derived by Hartzell and Heaton (1986) from the inversion of strong motion waveform data. The large dot denotes the hypocenter and the stippled region denotes the approximate region that is slipping at a particular instant in time.

after the passage of the rupture front. This class of models is usually referred to as 'dislocation models' and slip duration is synonomous with dislocation rise time. The spatial distribution of the slip amplitude is varied to give an acceptable match to the observed waveforms. In some of these models the dislocation rise time is assumed to be uniform on the rupture surface, and in others it is allowed to vary spatially to improve the quality of the fit. In principal, dislocation models can be parameterized with enough flexibility to encompass all possible slip histories on a fault surface (including those that result from dynamic 'crack-like' rupture

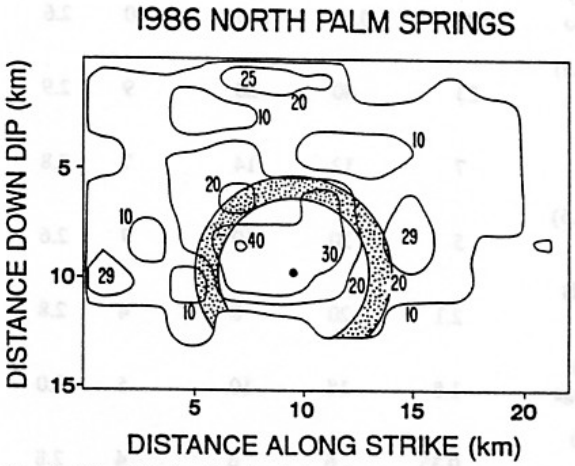

Fig. 6. Slip distribution (cm) for the $M = 6.0$ 1986 North Palm Springs, CA, earthquake derived by Hartzell (1989) from the inversion of strong motion waveform data. The large dot denotes the hypocenter and the stippled region denotes the approximate region that is slipping at a particular instant in time.

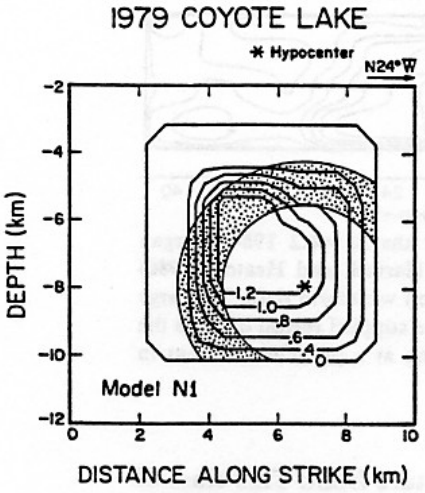

Fig. 7. Slip distribution from the $M = 5.9$ 1979 Coyote Lake, CA, earthquake derived by Liu and Helmberger (1983) from modelling strong motion waveform data. The stippled region denotes the approximate region that is slipping at a particular instant in time.

models), although most applications of dislocation models assume that the duration of slip is relatively homogeneous on the fault surface.

Several functional forms for the slip time history have been tried, the simplest being a simple ramp of duration T_s. However, more complex functional forms have been tried. For instance, a slip that grows as the square root of time has also been used (e.g. Beroza and Spudich, 1988), although slip histories of this form have not satisfactorily matched observed waveforms. Because these models were not constructed to match high-frequency data, details of the slip history cannot be derived. Instead, the models give an indication of how much slip occurs within a given time after the passage of the rupture front.

Table 1 gives a comparison of dislocation rise times T_s derived from these models with dislocation rise times that would be expected if the

TABLE 1

Observed rupture parameters

Earthquake	Moment ($\times 10^{25}$ dyn cm)	l (km)	w (km)	l_A (km)	V_r (km s^{-1})	$\frac{2\sqrt{S}}{3V_r}$ (s)	$\frac{2l_A}{3V_r}$ (s)	T_s (s)	Reference
19/9/88 ($M = 8.1$) Michoacan, Mexico	1500	150	120	~40	2.6	33	10	5	Mendoza and Hartzell (1989)
28/10/83 ($M = 7.3$) Borah Peak	23	40	20	9	2.9	6.5	2.1	0.6 [a]	Mendoza and Hartzell (1988)
9/2/71 ($M = 6.5$) San Fernando [b]	7	12	14	7	2.8	3.1	1.9	0.8	Heaton (1982)
15/10/79 ($M = 6.5$) Imperial Valley	5	30	10	7	2.6	4.5	1.8	1.0	Hartzell and Heaton (1983)
24/4/84 ($M = 6.2$) Morgan Hill	2.1	20	8	4	2.8	3.0	1.0	0.3	Hartzell and Heaton (1986)
8/7/86 ($M = 6.0$) North Palm Springs	1.8	18	10	5	3.0	3.0	1.1	0.4 [c]	Hartzell (1989)
6/8/79 ($M = 5.9$) Coyote Lake	0.35	6	6	4	2.8	1.4	0.9	0.5 [d]	Liu and Helmberger (1983)

[a] From teleseismic data; may be as large as 1 s.
[b] Estimates are for the first of two sources.
[c] A maximal value, may have actually been shorter.
[d] A maximal value, may actually have been shorter. Bouchon (1982) modeled this data assuming an instantaneous rise time.
l, approximate rupture length; w, approximate rupture width; l_A, approximate dimension of the major asperity; V_r, average rupture velocity; S, rupture area (lw); T_s, observed dislocation rise time.

duration of slip is comparable to the overall rupture duration of the earthquake. In many instances, the estimate of the rise time from these models is a maximum number since the data was low-pass filtered. Although dislocation rise time is one of the most difficult numbers to extract from deterministic source models, it would be very difficult to exceed the rise time estimates given in Table 1 by a factor of 2. However, in many instances, it would be possible to use significantly shorter slip durations. Several estimates of characteristic rupture length dimensions for the earthquakes are also given in Table 1. In many instances the slip distribution is spatially heterogeneous and therefore the characteristic dimension l_A of the dominant asperity for each earthquake is also given.

Two predictions of the dislocation rise time are given assuming that the slip duration is comparable to the time required for rupture. These predictions are based on the assumption that information must reach a given point on the fault about the final dimensions of the rupture surface. In the first it is assumed that the dislocation continues until information is received that the entire fault has ruptured, in which case the rise time T_s is approximately given by eqn. (5). In the second, the dislocation rise time is assumed to be comparable to the time required to rupture the dominant asperity, in which case we would expect the dislocation rise time to be approximated by

$$T_s \approx \frac{2l_A}{3V_r} \qquad (6)$$

Other methods for estimating the expected dislocation rise time can be devised. For instance, the fault width may be the most appropriate dimension for long, narrow rupture surfaces. However, for the fault models shown, the rupture widths are of the same order as rupture lengths and the widths are larger than the dimension of the dominant asperity. Furthermore, we might expect the slip duration to be highly variable over the rupture surface, with long rise times in the center of faults and short rise times near the rupture boundaries. A more complete estimate for expected slip durations would require specific dynamic rupture models for the earthquakes considered. At this point, however, I simply wish to test the hypothesis that the slip duration at any point is comparable to the time required for overall rupture.

As can be seen in Table 1, the rise times derived from modeling data are, on average, only 16% as long as that expected from the overall rupture duration (eqn. 5) and 42% as long as that expected from the rupture duration of the dominant asperity (eqn. 6). Kanamori and Anderson (1975) also reported comparably short dislocation rise times based on a completely different data set. We are led to the rather surprising conclusion that only a small portion of the overall rupture surface is undergoing slip at any given point in time. This is shown graphically in Figs. 1–7; the stippled bands represent the approximate area slipping at one instant in time. We can imagine that the rupture is actually a propagating pulse of slip that covers only 10% of the rupture surface at any point in time. The size of the slip in this pulse rises and falls as the rupture proceeds along the fault surface.

This model of earthquake rupture as a propagating pulse of slip is very similar to the simple model introduced by Haskell (1964) 25 years ago to estimate the energy radiated by earthquakes. Haskell found that relatively short dislocation rise times were necessary to account for the relatively large radiated energy from earthquakes. Brune (1970), qualitatively introduced a similar self-healing slip-pulse model to explain apparent discrepancies between 'effective stress' estimated from the spectral content of radiated seismic waves and static stress drops. Brune called this the 'partial stress-drop' and 'abrupt locking' model and this model has been suggested to explain the radiation from aftershocks of the 1971 San Fernando, California, earthquake (Tucker and Brune, 1977) and from small earthquakes near Anza, California (Brune et al., 1986).

Other evidence is now presented in support of short slip durations. The first is eye witness reports of the scarp formation of the M7.3, 1983 Borah Peak earthquake. The time required to propagate a rupture front along the 40-km length of this earthquake exceeded 10 s. Wallace (1984) documented the recollections of Lawana Knox who was about 300 m from the surface trace of

the earthquake. According to Wallace, "Mrs. Knox reported that the 1- to 1.5-meter-high scarp formed in about 1 s. She reported that the scarp reached its full height quickly, and that it did not appear to adjust up or down later or oscillate up and down while reaching its full height". This short rise time was independently corroborated by the account of two other eyewitnesses (Pelton et al., 1984) and is remarkably close to the value used by Mendoza and Hartzell (1989).

Some may argue that seismic modeling is sensitive only to the high dislocation particle velocities at the rupture front and that seismic waves are not sensitive to the long-period slip that occurs after the rupture front passes through. However, Beroza and Spudich (1988) attempted to model the 1984 Morgan Hill earthquake with just such a model. Following the model of Kostrov (1966), they used a dislocation time history that varies as the square root of time. This produces a time function with a very sharp rise and a very smooth tail. Yet in order to fit the strong motion records, they were forced to truncate the slip function after a mere 0.2 s, an even shorter dislocation rise time than that deduced by Hartzell and Heaton (1986).

As a final example, consider the strong ground motions recorded during the 1985 Michoacan earthquake. Anderson et al. (1986) showed that ground displacements (relative to an inertial frame) could be deduced from the ground acceleration records. They showed that observed static sea-level changes coincide with the ground displacement inferred from strong motion records. Furthermore, these static deformations occurred within a relatively short time period, and they cited this as evidence in support of the Brune 'partial stress drop' model (short slip duration). Mendoza and Hartzell (1989) modeled teleseismic body waves and the long-period ground velocity (with respect to an inertial frame) in the near-source region and found that this data required short dislocation rise times (< 5 s for a $M8.1$ earthquake). Comparisons of the observed displacements with those synthesized by Mendoza and Hartzell (1989) are shown in Fig. 8. A dislocation rise time comparable to the rupture time would effectively double the length of the synthetic records. In Fig. 8, notice that the motion at CAL (near the epicenter) has

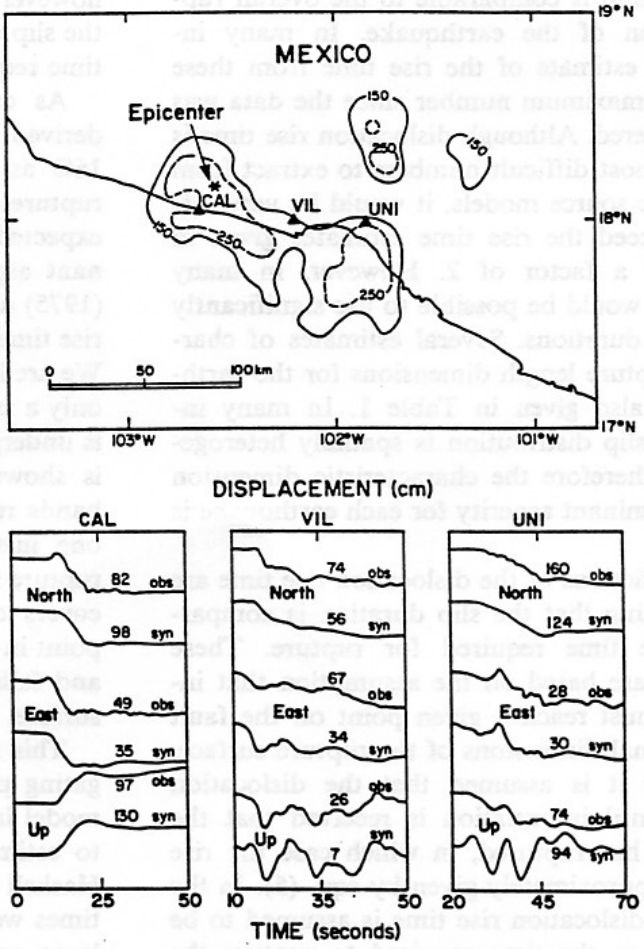

Fig. 8. Comparison of ground displacements (with respect to an inertial frame) observed above the 1985 Michoacan earthquake with displacements synthesized from the rupture model of Mendoza and Hartzell (1989). The observed vertical displacement at Caleta de Campos (CAL) coincided with locally observed sea-level changes (Anderson et al., 1986), indicating that the final static displacement was obtained within the 10-s interval inferred from the displacement record. The rupture surface is approximately 30 km below the stations and most of the duration of the record is due to the finite time required for the rupture to propagate and for the waves to arrive from different parts of the fault. If the dislocation rise time was comparable to the rupture time, then the duration of the records would be considerably longer.

stopped before it even begins at UNI which is located near the southern end of the rupture.

Ruppert and Yomogida (1990) also investigated the ground displacement at CAL and they concluded that it was best explained by a 'crack-like' model in which the slip duration is variable on the

rupture surface and is controlled by the overall rupture dimension. In order to produce the short-duration ramp-like displacement at CAL, Ruppert and Yomogida (1990) propose bilateral rupture (i.e. both up- and down-dip) on a fault width of < 40 km which results in slip durations of < 6 s and 8-m dislocations in the hypocentral region. This slip duration is roughly comparable with that deduced by Mendoza and Hartzell (1989), but they used considerably larger fault dimensions and inferred smaller dislocations to model a much larger set of data.

In summary, there are a number of observations that suggest that the slip duration at a given point on a fault is short compared with the time required for information to travel from the boundaries of the rupture. However, because the slip duration must be inferred from interpretations of rupture models, I believe that it is not yet possible to consider this as a proven hypothesis. If, in fact, the dislocation rise times are not short compared with the overall rupture time for earthquakes, then there are many earthquake models determined from waveform data that have seriously underestimated the slip for earthquakes. For the remainder of this paper, it is assumed that slip durations are indeed short relative to the overall rupture duration. Physical mechanisms that are compatible with both a short slip duration and also a correlation between average slip and overall rupture dimensions will be discussed later.

3. Stress in time and space

Several estimates of stress are now discussed that can be obtained from the earthquake models used in this study. In large part, these stress estimates are obtained by estimating strain variations (spatial derivatives of displacements). Measures of stress can vary considerably depending upon the details of the slip history; details that are only poorly resolved by waveform modeling studies. Nevertheless, it is possible to get some idea of the order of magnitude of stress and strain variations implied by the rupture models considered in this paper.

The static stress drop for a rupture can be calculated by first assuming that the rupture surface is free to slip along the fault plane; tractions are then applied parallel to the rupture surface such that they reproduce some distribution of slip. These tractions are averaged over the rupture surface to give an average static stress drop $\overline{\Delta\sigma}$ for an earthquake. Since all of the equilibrium equations for stress and strain are linear functions of D, the estimate of the static stress drop only depends on the final distribution of slip and is independent of how the slip actually occurred in time. Several solutions have been derived for the slip distribution that would result if the stress drop is uniform. Eshelby (1957) derived the following stress drop for a circular fault in a Poissonian whole space.

$$\Delta\sigma = 0.78\mu\frac{\overline{D}}{\sqrt{S}} \tag{7}$$

Stress drops have also been numerically computed from the average slip assuming rectangular faults at various depths of burial in an elastic half-space by Parsons et al. (1988) and their results can be summarized by

$$\Delta\sigma = C\mu\frac{\overline{D}}{L} \tag{8}$$

where L is either the fault length l or width w and C is a constant that can have values between 0.65 and 2.55 depending upon the ratio of l to w, the rupture depth, and the slip direction.

Das (1988) investigated the relationship between static stress drop averaged over the rupture surface $\overline{\Delta\sigma}$ and average slip D for models in which the stress drop is spatially heterogeneous and concluded that eqn. (8) is not strongly dependent on the spatial distribution of the stress drop, i.e. it is usually valid to approximate the average stress drop from a heterogeneous stress distribution assuming eqn. (8). When the slip distribution is significantly heteorgeneous, the stress drop may actually be negative on some parts of the rupture surface, i.e. an area of low slip that is surrounded by areas of high slip may have a higher stress after the rupture than it did before.

Static stress drop estimates are given in Table 2 for the seven earthquakes. For simplicity, the average stress drop $\overline{\Delta\sigma}$ is calculated assuming a circular rupture in a whole space (eqn. 7). The aver-

TABLE 2

Estimates of stress

Earthquake	$\sqrt{S}$ (km)	l_A (km)	l_p (km)	$\overline{D}$ (cm)	D_{max} (cm)	$\overline{\Delta\sigma}$ (bars)	$\Delta\sigma_A$ (bars)	$\overline{\Delta\sigma_p}$ (bars)	$\Delta\sigma_{Ap}$ (bars)
19/9/88 ($M = 8.1$) Michoacan	134	40	13	238	650	5	29	14	37
28/10/83 ($M = 7.3$) Borah Peak	28	9	2 [a]	82	147	8	30	26	46
9/2/71 ($M = 6.5$) San Fernando [b]	13	7	2	120	250	25	65	40	84
15/10/79 ($M = 6.5$) Imperial Valley	17	7	2.7	48	180	8	47	13	50
24/4/84 ($M = 6.2$) Morgan Hill	13	4	0.8	38	100	8	45	32	84
8/7/86 ($M = 6.0$) N. Palm Springs [c]	13	5	1.2 [d]	26	45	6	18	12	22
6/8/79 ($M = 5.9$) Coyote Lake [e]	5	4	1.4 [f]	46	120	22	48	22	57
					Lognormal average	9.8	37	20.7	49.5

[a] From teleseismic data, may be as large as 3.
[b] Estimates are for the first of two sources.
[c] μ assumed to be 3.9×10^{11} dyn cm^{-2}.
[d] A maximal value, may actually have been smaller.
[e] μ assumed to be 3.1×10^{11} dyn cm^{-2}.
[f] A maximal value, may actually have been smaller.

l_p, length of the rupture pulse ($V_r T_s$); $\overline{D}$, average dislocation ($\frac{M_0}{S\mu}$; $\mu = 3.5\times10^{11}$ dyn cm^{-2}); D_{max}, peak dislocation; $\overline{\Delta\sigma}$, average static stress drop; $\Delta\sigma_A$, static stress drop in the vicinity of the dominant asperity; $\overline{\Delta\sigma_p}$, average dynamic stress drop in the vicinity of the rupture pulse; $\Delta\sigma_{Ap}$, dynamic stress drop of the rupture pulse at the dominant asperity.

age dislocation $\overline{D}$ is calculated from the moment estimates assuming the given rupture area S and a rigidity of 3.5×10^{11} dyn cm^{-2}. Static stress drops $\Delta\sigma_A$ for the dominant asperity are also given, where $\Delta\sigma_A$ was calculated using the assumption that

$$\Delta\sigma_A \approx 0.52\mu\frac{D_{max}}{l_A} \quad (9)$$

where D_{max} is the peak slip and l_A is the approximate diameter of the dominant asperity. Equation (9) assumes uniform stress drop over a circular crack and is similar to eqn. (7) except that it is computed using the peak displacement instead of the average displacement (Eshelby, 1957). Of course, these are very rough estimates of the static stress drop and higher stress drop estimates are expected for models in which the slip distribution is elongated in a direction.

The static stress drops provide some estimate of the overall change in stress state on the ruptured surface. However, it has been hypothesized that slip occurs in a narrow pulse that propagates along the rupture surface, and therefore we can anticipate that there are larger transient stress changes in the vicinity of the propagating slip pulse. Calculation of these stress changes in the vicinity of the slip pulse must be made by assuming a detailed model of the conditions on the fault during slip. As pointed out by Freund (1979), the stress from a propagating crack is a function of the rupture velocity. Calculation of these stress variations for the models used in this paper is a formidable task that is beyond the scope of this study. Furthermore, the details of the slip history are not sufficiently resolved by these models to warrant such calculations. However, it is possible to obtain some insight into this problem by examining a very simple model of a pulse of slip that propagates steadily along a fault surface.

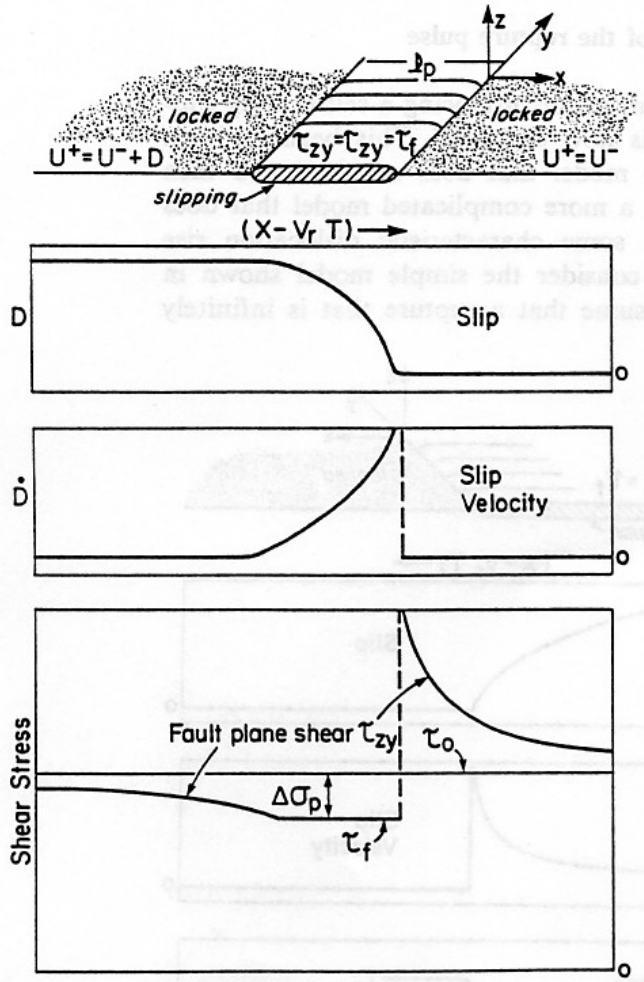

Fig. 9. Idealized model of Freund (1979) in which a pulse of slip of length l_p in the x-direction and infinitely wide in the y-direction propagates steadily at velocity V_r in the positive x-direction. A uniform shear stress $\tau_{yz} = \tau_0$ is applied at infinity and the shear stress on the slipping portion of the fault is assumed to be uniformly equal to a dynamic friction τ_f. In this model, the slip is confined to a pulse artificially, i.e. there is no physical condition that causes the rupture to heal. Because the problem is steady-state, the pulse causes a finite dislocation that propagates over an infinitely large fault and thus the static stress drop is zero. The dynamic stress drop in the pulse $\Delta\sigma_p$ is a function of the dislocation and the length of the slip pulse, and is given by eqn. (10).

Freund (1979) gives the solution for a pulse of slip that propagates steadily at velocity V_r along the x-axis assuming that a homogeneous shear stress τ_0 is applied from infinity. In this model (shown in Fig. 9), the fault is assumed to be welded everywhere, except in a strip of length l_p in the x-direction and infinitely wide in the y-direction, that propagates steadily along the x-axis. The shear stress across the slipping part of the fault is assumed to be uniformly equal to τ_f. As can be seen in Fig. 9, the stress on the fault changes dramatically with respect to the location of the slip pulse. There is a square root singularity at the leading edge of the slip pulse. One measure of the dynamic stress change in this model is the shear stress applied at infinity minus the shear stress on the slipping strip of the fault which is referred to as $\Delta\sigma_p$, given by Freund (1979) as

$$\Delta\sigma_p = \tau_0 - \tau_f = \frac{\mu}{\pi}\frac{D}{l_p}\sqrt{1-\frac{V_r^2}{\beta^2}} \qquad (10)$$

where β is the shear-wave velocity and $l_p = V_r T_s$ is the length of the slipping region. If the rupture velocity is assumed to be 80% of the shear-wave velocity, then $\Delta\sigma_p = 0.19\,\mu D/l_p$. It should be noted that this definition of stress drop is similar in form to eqn. (8) for static stress drops, but with a small value for the geometric constant C. In fact, since Freund's (1979) solution is steady state, it can be solved as a static problem superposed on a moving coordinate system. As a consequence of this steady-state condition, this solution does not radiate seismic waves to the far field (even though there is an infinitely large stress change at the crack tip). Another unusual feature of this model is the fact that the static stress drop is zero, i.e. the stress at large distances behind the propagating slip pulse is the same as the stress at large distances ahead of the slip pulse. Furthermore, notice that as the rupture velocity approaches the shear-wave velocity, a pulse with an arbitrarily large slip will propagate with an arbitrarily small dynamic stress drop $\Delta\sigma_p$. Because there are many non-physical consequences of the restrictive assumptions of Freund's model and because the length of the estimated slip pulse l_p is an upper bound in many of the slip models, I expect that the dynamic stress drop given by eqn. (10) gives a lower bound on the dynamic stress drops implied by the slip models shown in Figs. 1–7.

Estimates of the average dynamic stress drop $\overline{\Delta\sigma_p}$ in the vicinity of the rupture pulse are given in Table 2. The average dislocation $\overline{D}$ is used in eqn.

(10) to calculate the dynamic stress drop $\overline{\Delta\sigma_p}$ in the slip pulse averaged over the rupture, and the maximum dislocation D_{max} is used to calculate the stress drop $\Delta\sigma_{Ap}$ in the slip pulse in the region of the dominant asperity. The logarithmically averaged (the antilog of the average of the logarithms) dynamic stress drop in the vicinity of slip pulses $\overline{\Delta\sigma_p}$ is 21 bars, whereas the average static stress drop $\overline{\Delta\sigma}$ is only 9.8 bars. Thus, according to this very simple steady-state model, the dynamic stress drop (the difference between the ambient shear stress and the shear stress at the slip pulse) is several times larger than the static stress drop (in Freund's model, the static stress drop $\Delta\sigma$ is zero).

Dynamic stress drops $\Delta\sigma_{Ap}$ are also calculated in the vicinity of the dominant asperities (Table 2) using eqn. (10) together with the estimated length of the slip pulse and the maximum slip in the asperity. Unfortunately, the assumptions used to derive eqn. (10) are severely taxed for this calculation, i.e. the length of the slip l_p is, on average, only one third the average dimension of the dominant asperity. Whereas in Freund's model, the slip is assumed to be infinitely wide along the rupture front and it is assumed to propagate uniformly an infinite distance in the x-direction (thereby resulting in zero static stress drop). In the vicinity of the dominant asperity, application of eqn. (10) yields an average dynamic stress drop $\Delta\sigma_{Ap}$ of 50 bars, whereas the static stress drop $\Delta\sigma_A$ averages 37 bars. However, it is important to recognize that these numbers are based on very crude models. Until more realistic numerical models are available to estimate the dynamic stresses implied by rupture models such as those shown in Figs. 1–7, I can only speculate that the dynamic stress drop in the region of the dominant asperities is greater than the static stress drop, but less than several times as large. Of course the stress just ahead of the leading edge of the rupture can be much larger and presumably is limited by the overall strength of the materials in the fault zone. Furthermore, if the rupture propagates smoothly, then there is no far-field radiated energy and thus the ultimate amplitude of the stress change in the vicinity of the crack front cannot be deduced from observations of radiated high-frequency waves.

4. Healing of the rupture pulse

A mechanism for producing a self-healing rupture pulse is now discussed. This begins with a very simple model that does not heal and then proceeds to a more complicated model that does heal within some characteristic dislocation rise time. First consider the simple model shown in Fig. 10. Assume that a rupture that is infinitely

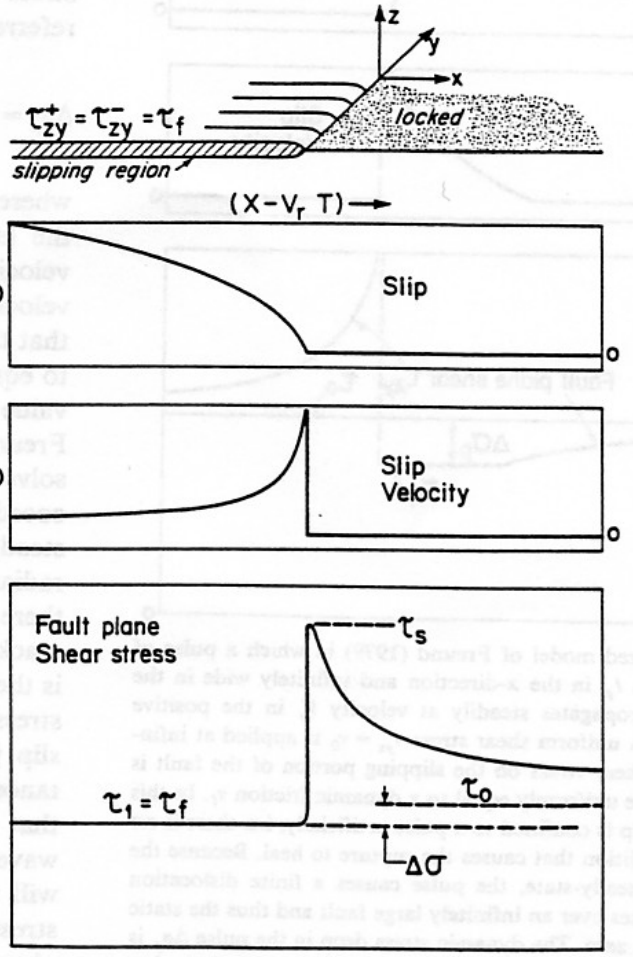

Fig. 10. Idealized model of a rupture (infinitely wide in the y-direction) propagating at a velocity V_r in the x-direction. Fracture initiates when the stress at the crack tip exceeds the static strength of the fault τ_s and the stress on the fault behind the crack tip is some constant frictional level τ_f. The stress before the initiation of rupture is τ_0 and the stress after the rupture is $\tau_1 = \tau_f$, giving a stress drop of $\Delta\sigma = \tau_0 - \tau_f$. This type of rupture is described by Kostrov (1966) and the dislocation continues to grow as $\sqrt{V_r t - x}$ and does not heal until information is received that the rupture front has stopped propagating.

long in the y-direction is propagating uniformly at a rupture velocity V_r in the x-direction. The shear stress on the fault τ_{zy} is assumed to be τ_0 at a large distance in front of the rupture and τ_1 at a large distance behind the rupture, giving a static stress drop $\Delta\sigma$ of $\tau_0-\tau_1$. In the region ahead of the rupture, the shear stress τ_{zy} is assumed to be given by crack theory and to be less than some critical strength τ_s. In the region behind the rupture front, the shear stress is equal to a friction stress τ_f that is constant in time once the fault has ruptured. If this model applies to earthquakes, then the fact that average static stress drops are only tens of bars allows us to conclude that the frictional stress τ_f has an amplitude that is close to the ambient shear stress. Furthermore, experimental studies of rock friction indicate that the coefficient of friction for a sliding surface is within several percent of the static coefficient of friction (Dieterich, 1979). if the coefficient of friction is somewhere near 0.6 (typical for rocks in laboratory experiments), then we conclude that for the model in Fig. 10, all of the shear stresses plotted would be in the kilobar range, and any variations in the stress would be relatively small compared with the ambient tectonic shear stress.

The dislocation D is zero ahead of the crack tip and in the region behind the crack tip it is given by

$$D = f(\Delta\sigma)\sqrt{V_r t - x} \tag{11}$$

where the function f depends upon the stress drop and the elastic properties of the medium. The slip velocity $\dot{D}(V_r t - x)$ is given by

$$\dot{D} = \frac{f(\Delta\sigma)V_r}{2\sqrt{V_r t - x}} \tag{12}$$

The slip on the fault continues to increase until the growth of the rupture is arrested. Models of this type produce dislocation rise times that depend upon the final dimensions of the rupture surface. A review of these types of models can be found in Aki and Richards (1980, chap. 15).

If dislocation rise times are short compared with the overall duration of the rupture, as is suggested from the modeling of seismic waves, then some other model for the rupture process must be considered. Dynamic rupture models in which the rupture heals before the rupture terminates are relatively rare. Yoffe (1960) presented such a model for a plane-strain extensional fracture, but the healing condition was artificially imposed and several key features of Yoffe's model are physically unrealistic. Similarly, Freund's (1979) model discussed in the last section (Fig. 9) features a self-healing pulse of slip that propagates steadily along a fault. However, the healing is merely introduced as a boundary condition and there is no physical process included to determine when the healing should occur.

Day (1982) constructed finite-element models of dynamic rupture on finite faults having stress boundary conditions on the fault that are similar to those in Fig. 10, i.e. the shear stress τ_{zy} is limited to be a constant value τ_f once rupture has occurred. Day also added the following condition; if the shear stress on the fault becomes less than τ_f then the rupture heals itself. With this type of boundary condition, Day shows that, in some circumstances, the rupture can heal itself before the rupture process terminates. In particular, for a long, narrow rupture of width w (the rupture is confined both above and below), Day shows that the dislocation rise time approaches a value of $w/2V_r$ as the rupture propagation approaches a steady state. In some ways it is surprising that Day's (1982) simple model produces a healing time that is so short, since the rupture heals while the leading edge of the rupture is only half of a fault width away. In a pseudo-static crack problem, the slip would continue to grow as the rupture front extends. S. Day (personal communication, 1989) attributes this rapid healing to overshoot of the slip (with respect to the static problem) caused by the momentum of the sides of the fault during the rupture process. The rapid healing in Day's (1982) model only appears for steady rupture along a long, narrow fault. When Day assumed a square fault with a radially spreading rupture front, the dislocation rise time was comparable to the rupture time.

Archuleta and Frazier (1978) constructed dynamic finite element rupture models for a vertical semi-circular fault in a half-space and stress boundary condtions on the fault identical to those

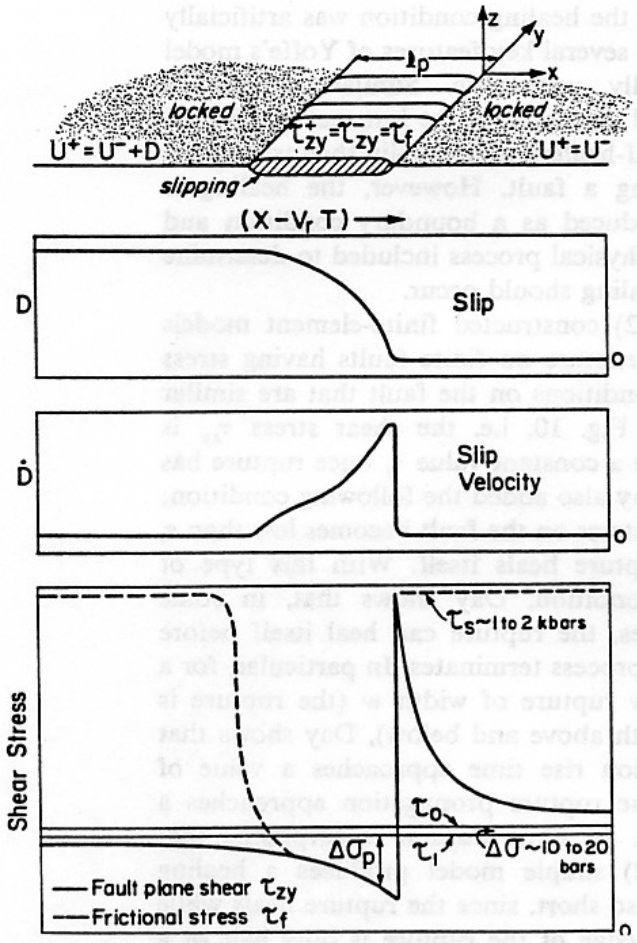

Fig. 11. Idealized model of a self-healing rupture pulse (infinitely wide in the y-direction) propagating at a velocity of V_r in the x-direction. Fracture initiates when the stress at the crack tip exceeds the static strength of the fault τ_s (~ k bar) and then drops to a sliding frictional level that is inversely proportional to the dislocation particle velocity $\dot{D}$. Dislocation particle velocities are high and sliding friction is very low (< 200 bars) near the rupture front. As the dislocation particle velocity decreases away from the rupture front, the sliding friction increases and the fault heals itself. In this simple model, the strength of the fault returns to a high level immediately after the rupture. τ_0 is the stress before the initation of rupture and τ_1 is the final stress after rupture has terminated, yielding a static stress drop $\Delta\sigma = \tau_0 - \tau_1$, which may be very low (~ 10 bars) depending on the final length of the rupture. The average stress drop locally within the rupture pulse may be considerably larger (~ 100 bars) with dislocation particle velocites in the range of 1m s^{-1}. The dislocation amplitude D and the length of the slip pulse l_p may be a sensitive function of the friction law during slip.

just described. They show that if the hypocenter is located at the bottom edge of the fault, then short slip durations can occur for points where the fault breaks the free surface of the half space. This short duration is attributed to overshoot of the slip with respect to static equilibrium as the dynamic rupture breaks the free surface. However, this short slip duration is only seen in special cases of Archuleta and Frazier's models, and in all cases that they considered, points interior to the rupture boundaries have long slip durations.

Spatially complex distributions of stress and strength introduce shorter length scales and it should be possible to construct hypothetical models that have short slip durations for at least some points interior to the boundaries of the rupture surface. However, if the average slip in such models is determined by the overall dimension of the rupture surface, then average slip durations are expected to be long, despite the introduction of shorter length scales. Chen et al. (1987) show numerical examples of the slip history for a dynamic fault model in which the stress drop is spatially heterogeneous (but positive everywhere in the rupture surface). Although the slip history becomes complex in their models, the duration of slip is still comparable to the overall duration of the rupture.

One way to make the slip duration short at a given point is to introduce barriers. That is, an earthquake consists of a number of short-duration, crack-like ruptures on small rupture areas that are separated by locked regions (Aki, 1979; Papageorgiou and Aki, 1983a,b). Barrier models differ from the heterogeneous stress drop models of Chen et al. (1985) in that there are actually locked patches remaining throughout the rupture surface. Large shear stress accumulates in these locked patches as the rupture propagates around them, effectively resulting in large negative stress drops in the barriers. Although barrier models can produce short slip durations, it appears that slip is relatively smoothly distributed in many of the earthquake models shown in Figs. 1–7, and yet, the duration of slip is short.

Are there physically reasonable ways to rapidly heal the rupture before information arrives that the rupture has stopped propagating? The stress

distribution in the slipping region may be the key. Brune (1970, 1976) suggested that earthquake rupture may be analogous to the propagation of dislocations in crystals where a localized slip propagates through a crystal lattice (for example, see Nabarro, 1967). Brune further suggested that a self-healing rupture pulse would result if the frictional stress τ_f is limited to some relatively low value immediately behind the rupture front but is then allowed to assume relatively high values at some finite distance behind the rupture front. A simple way to accomplish this is to assume that the friction stress τ_f is inversely related to the slip velocity $\dot{D}$ at any point on the fault. A slip-velocity-weakening friction law for faults was suggested by Burridge and Knopoff (1967) who numerically simulated earthquake rupture by assuming that a fault could be modeled as a system of discrete masses, coupled by springs, and sliding over a rigid surface. Their simulations did produce self-healing, propagating rupture pulses, although they did not emphasize the significance of such behavior.

One simple hypothesis would be to assume that the frictional stress on the fault τ_f is approximated by

$$\tau_f = \tau_s - a\dot{D} \tag{13}$$

where τ_s is a static friction and a is a material constant. A simple model of this type is shown in Fig. 11. In this model, slip only occurs if the shear stress on the fault $\tau_{zy} = \tau_f(\dot{D})$, and if $\tau_{zy} < \tau_f(\dot{D})$, then the fault is locked. As was the case in the previous simple model (Fig. 10), the dislocation is assumed to vary as $\sqrt{V_r t - x}$ in the region behind the rupture front and thus the dislocation velocity has an inverse square root singularity. The dynamic friction on the fault τ_f drops dramatically in the region immediately behind the crack tip and then increases as the square root of distance behind the rupture front. The rupture heals itself at a distance l_p behind the rupture front when τ_f exceeds the ambient stress on the fault. As is the case with most crack models, the square root singularities at the rupture front result in some non-physical artefacts such as infinite strains (derived from infinitesimal strain approximations), infinite particle velocities, and even more infinite particle accelerations. The infinite dislocation particle velocity, when used in conjunction with eqn. (13), forces τ_f to actually go infinitely negative at the rupture front. Thus, when thinking of the behavior of these models at the rupture front, the square root singularity should be taken to mean that strains may become very large, but they must be finitely bounded. In particular, the shear stress on the fault cannot exceed the yield strength of the fault, and dynamic friction τ_f cannot be negative.

S. Day (personal communication, 1989) has constructed finite element models of dynamic rupture assuming the velocity-dependent friction law given by eqn. (13). He reports that such a friction law can produce a self-healing pulse of slip that propagates along a rupture surface, although the stable propagation of such pulses occurs only for specific ranges of the constant a which determines the degree of slip velocity weakening.

Is there any physical basis for a dynamic friction of the type assumed in eqn. (13)? One simple hypothesis is that the friction on the fault is related to the normal stress across the fault surface τ_{zz}. In idealized planar fault models, the normal stress τ_{zz} is constant across the fault throughout the rupture process. That is, the fault plane is assumed to be a perfect node for P-waves. However, if there are geometric irregularities in the rupture surface or spatial variations in elastic properties in the vicinity of the rupture surface, then the fault plane will no longer be a perfect node for P-waves. In fact, observations of the high-frequency P-waves in the near-source region usually yield a fairly isotropic P-wave radiation pattern (Liu and Helmberger, 1985). If there are large-amplitude variations in the normal stress τ_{zz} in the rupture region, these will almost certainly have some effect on the effective frictional strength of the fault. Since the amplitude of high-frequency radiated waves is proportional to the dislocation velocity $\dot{D}$, it might be expected that the dynamic friction is a function of the slip velocity.

Brune et al. (1989, 1990) have studied spontaneous stick-slip failure in foam rubber and have documented that variations in normal stress on the slipping surface are responsible for slip-velocity-weakening friction. They found that when thin strips of foam rubber are mounted to rigid surfaces and then forced to slide, the sliding friction is the

same as the static friction. However, when the surrounding medium is entirely foam rubber, then significant normal stresses are observed in the vicinity of the sliding region and the apparent sliding friction is reduced. Tolstoi (1967), Oden and Martins (1985) have argued persuasively that dynamic variations in normal stress are of primary importance in determining the dynamic behavior of dry friction in metals.

If irregularities occur on a very small scale, then it may be that high-intensity, high-frequency compressional waves may exist in the immediate vicinity of propagating rupture pulses in earthquakes. Melosh (1979) discusses a model of this type that he calls '*acoustic fluidization*'. He shows that very high-frequency acoustic waves may be a reasonable mechanism for producing slip-velocity-weakening behavior that dramatically reduces frictional stress during fault rupture. If such compressional waves are to significantly reduce the confining stress on the rupture surface, then their intensity would have to be some significant fraction of the confining stress (on the order of kilobars for seismogenic depths). If this explanation is appropriate, then it may only be valid for ruptures that propagate within specified ranges of confining pressure and dislocation particle velocities.

Sibson (1973) and Lachenbruch (1980) discuss an alternative model for decreasing frictional stress during rupture. They propose that frictional stress may be dramatically reduced during rupture by the expansion of pore fluid caused by frictional heating. They suggest that frictional stress could be reduced from the range of kilobars to hundreds of bars as pore fluids rapidly heat during fault slip. Lachenbruch (1980) suggests that the pore fluid pressure may rapidly dissipate by the propagation of hydrofractures thereby causing re-strengthening of the fault. The time required for this re-strengthening could range from seconds to years depending upon the characteristics of the fluid flow.

5. Consequences of self-heating rupture

There are some interesting implications that result from a model of the type shown in Fig. 11. The constant a, which controls the slip velocity weakening in the friction law (eqn. 13), has a fundamental effect on the rupture. If a is large, then the length l_p of the rupture pulse is large and so is the dislocation. If a becomes small, then the dynamic friction increases and rupture stops. The length of the slip pulse and size of the dislocation in the slip pulse rises and falls as it proceeds down the fault, depending on the relative amplitude of the ambient stress τ_0 and the dynamic friction τ_f (which itself depends on the dislocation particle velocity). Because the slip velocity and the dynamic friction are dependent on each other, mathematical solutions for the slip are likely to be rather unstable with respect to assumed initial conditions. It is conceivable that the static strength τ_s and the ambient stress τ_0 may both be relatively homogeneous along a rupture that has a relatively irregular slip distribution, i.e. the slip distribution may be controlled by details of the behavior of the dynamic frictional strength in the region of the slip pulse. It might be difficult to recognize which segments of a fault may have large slips just by looking at physical samples of fault material.

The amplitudes of various stresses for the self-healing slip pulse model of Fig. 11 are now speculated upon. The static friction on the fault τ_s could be quite high, perhaps in the kilobar range, which is the inferred strength of materials at confining stresses appropriate for seismogenic depths. Yet since the dynamic friction during rupture τ_f may be relatively low (perhaps in the range of several hundred bars), the work done against friction during rupture may be relatively low, thus explaining the relatively low heat flow seen in the vicinity of the most active faults (Brune et al. 1969; Lachenbruch and Sass, 1973, 1980; Richards, 1976). The static stress drop, which is measured from the overall fault dimensions, may be much lower still (in the range of tens of bars). If propagation of a rupture pulse of a given slip amplitude is arrested in a relatively short distance, then a relatively high static stress drop results. If that same rupture pulse travels a long distance, then a relatively low static stress drop results.

In the slip pulse model, frictional heating is controlled by dynamic friction during rupture and not by the static friction τ_s. Heat flow measure-

ments apparently constrain the dynamic friction of the San Andreas fault to be less than several hundred bars. Furthermore, the very rough estimate of dynamic stress drops $\Delta\sigma_p$ from the earthquakes considered in this paper (Table 2) leads me to guess that the ambient stress is usually no more than several hundred bars higher than the average dynamic friction. Therefore, the ambient shear stress on the San Andreas fault may be expected to be less than 400 bars. Zoback et al. (1987) also infer relatively low shear stresses on the San Andreas fault because many independent measurements imply that the maximum compression axis is nearly perpendicular to the fault. Of course, heat flow measurements do not constrain the dynamic frictional stress values for relatively low slip-rate faults. The existence of large mountains is convincing evidence that the ambient shear stress in the crust is in the range of a kilobar at some localities (Jeffreys, 1959).

Once a slip pulse has initiated, the ambient stress τ_0 necessary to support the propagation of large slip pulses may be considerably less than the static friction τ_s. Thus, sections of the fault that support large slip pulses would tend to be at an ambient stress that is low compared to the stress necessary to initiate rupture. This may explain why sections of the fault that have large coseismic slips tend to have low seismicity levels (the stress is too low to initiate rupture).

We see, then, that the slip pulse model allows for a large variation between the different measures of stress in the earthquake process. The static strength of the fault zone τ_s may be in the kilobar range; the ambient shear stress in the region of the earthquake may be lower but still quite high (perhaps in the range of hundreds of bars on very active faults to a kilobar on relatively inactive faults); the dynamic stress differences in the region of the rupture may be relatively high (in the range of tens to hundreds of bars in the slipping part of the fault to kilobars at the crack tip); the sliding friction during rupture τ_f may be relatively low (less than several hundred bars); and the final change in ambient stress (the static stress drop $\Delta\sigma$) may be very low (in the range of tens of bars).

If there is a region of small slip surrounded by regions of large slip, then in the region of small slip, the stress after the earthquake τ_1 may actually be higher than the stress before τ_0. In the case of the Morgan Hill earthquake, there was an extensive area of small slip between two regions of large slip (Fig. 5). Although behavior of this type can be understood in the context of the simple model of Fig. 10, it seems to imply a very heterogeneous distribution of either ambient or frictional stress. However, this behavior seems to follow naturally from the slip pulse model shown in Fig. 11. The slip pulse, which was less than a kilometer wide, propagated from north to south at a velocity of about 2.8 km s^{-1}. The size of the slip pulse was initially large, then diminished as it propagated southward and then grew relatively large again at the south end of the rupture. The small slip in the region between the asperities did not grow large when the second asperity broke because the fault had already become locked.

If indeed the slip pulse model is appropriate, then the ambient stress along many active faults may be much lower (perhaps by a factor of 0.20) than the stress necessary to initiate rupture and the problem of earthquake prediction becomes a problem of predicting when and where large slip pulses will propagate. Or restating the problem, we must know how to predict when a slip pulse will stop propagating (this problem is discussed in more detail by Brune, 1979). Since the static stress drop $\overline{\Delta\sigma}$ is small compared with other stresses involved in this model, prediction schemes that depend on static stress drop estimates (for instance the time-predictable or slip-predictable models; Shimazaki and Nakata, 1980) may not be appropriate. Even after a large earthquake, there may be sufficient ambient stress to support the propagation of another slip pulse. As an example, consider the apparent 6-m slips that occurred on the San Andreas fault at Pallett Creek in both 1812 and 1857, a mere 45 years apart (Salyards, 1989). Alternatively, a region may experience a long interseismic period simply because no slip pulses of large enough size propagated into the region (some interevent periods at Pallett Creek exceed 300 years; Salyards, 1989). If this is true, then even the approximate prediction of the time of large earthquakes may be difficult. Kagan and

Jackson (1990) report that mature seismic gaps as defined by McCann et al. (1979) had fewer large earthquakes in the period from 1979 to 1988 than recently filled seismic gaps.

In the introduction of this paper, it was noted that the average fault slip $\overline{D}$ correlates well with the square root of the rupture area for a wide variety of earthquakes (Kanamori and Anderson, 1975). If earthquake ruptures have approximately constant ratios of width and length, then this correlation implies that average static stress drops $\overline{\Delta\sigma}$ are approximately independent of the rupture dimension. However, Scholz (1982) argues that average dislocations correlate well with fault lengths, even for faults in which the apparent rupture width is small compared to the length. This observation is evidence that long, narrow ruptures tend to have higher static stress drops. However, in the slip-pulse model proposed here, the most natural explanation for a correlation between average dislocation and rupture length (regardless of the rupture width) is that pulses with very large slip tend to propagate large distances. If a very large slip pulse develops on a long, narrow fault (e.g. the San Andreas), it may run for a very large distance. This problem is discussed at some length by Bodin and Brune (1990).

For faults of a given aspect ratio (length to width ratio), the static stress drop is controlled by the distance that a slip pulse propagates. If for some reason, large slip pulses are arrested after relatively short rupture lengths, then high static stress drops would result. If the same size slip pulse does not stop, then a lower static stress drop would result, even if the dynamic behavior along the slip pulse was approximately the same. This suggests an interesting interpretation of the observation that geologic slip rates inversely correlate with static stress drop (Kanamori and Allen, 1986). That is, faults with the highest geologic slip rates tend to have earthquakes with relatively low static stress drops. If we assume the slip pulse model, then this implies that slip pulses with a given dislocation tend to travel larger distances on very active faults than they do on relatively inactive faults. Perhaps faults with high geologic slip rates tend to be long faults with relatively homogeneous properties that allow slip pulses to propagate large distances. Therefore, it is conceivable that the static strength of faults and the dynamic stresses during rupture may be relatively independent of geologic slip rate.

Although the model that has been presented may imply that it will be very difficult to predict the time of large earthquakes, it also implies that it should be possible to predict (at least statistically) the overall size of an earthquake soon after the rupture has initiated and well before the rupture stops. That is, since there is a well-established correlation between average dislocation and fault length, and because the final dislocation is reached quickly after the passage of the rupture front, it should be possible to recognize the dislocation size quickly. This would allow a statistical prediction of the rupture dimension before the rupture stops. This principle may be useful in real-time earthquake warning systems that are designed to provide very short-term predictions (seconds to tens of seconds) of strong ground shaking for sites located at large enough distances from the epicentral region (Heaton, 1985).

6. Nucleation of rupture

The slip pulse model shown in Fig. 11 assumes a running rupture pulse. Since in this model no slip pulse will propagate unless a slip pulse already exists, the model clearly begs the question of how the rupture pulse starts in the first place. A different class of models is necessary to trigger the initial slip instability (for example; Rice and Tse, 1986; Okubo, 1989). At what point (or earthquake size) does the physics that controls the rupture change from the nucleation process (for which inertia is not important) to the slip pulse process (where inertia is very important)? Presumably, this transition is related to the size of the rupture, and we would expect that the slip pulse model does not apply to earthquakes that are small enough. How small is that? Unfortunately, detailed rupture models have not yet been developed to study the relationship between rupture time and dislocation rise time for earthquakes smaller than about magnitude 5. However, the overall seismic radia-

tion from earthquakes down to at least magnitude 3 seems to be self-similar (assuming certain scaling relationships) with that of larger events (for example; Brune et at., 1986; Frankel and Wennerberg, 1989). Although this doesn't prove anything, it does suggest that the rupture pulse model may be applicable for relatively small earthquakes as well.

Presumably sections of faults that primarily creep do not support the propagation of slip pulses. For example, consider the creeping section of the San Andreas fault in central California. Whereas the locked Carrizo Plains section of the fault is devoid of seismicity, the creeping section has a high seismicity rate. One explanation is that the Carrizo Plains segment supports the propagation of large slip pulses that maintain the ambient stress at a relatively low level. However, the creeping section of the fault evidently does not support large slip pulses, thereby allowing the ambient stress to increase to a level sufficient to cause creep and the nucleation of numerous small ruptures that don't propagate very far.

A serious problem still exists with this interpretation. Laboratory measurements indicate that creep generally does not initiate until shear stresses are a substantial fraction of the confining stress (typically 0.4 to 0.6; J.H. Dieterich, personal communication). Since the notion of low dynamic friction in this model is not relevant to the problem of fault creep, I cannot claim that shear heating on creeping sections of the San Andreas fault is low because of low dynamic friction. Although there is a tendency for the heat flow to be somewhat high in the general region surrounding the central creeping section of the San Andreas fault (Lachenbruch and Sass, 1980), the heat flow is not localized to the fault and is not high enough to be compatible with kilobar shear stress levels on the creeping section of the fault (Brune et al., 1969). High fluid pore pressures that reduce the effective confining stress can be invoked to assert that the yield strength of the creeping fault may only be hundreds of bars. Unfortunately, I know of little corroborating evidence for this somewhat ad hoc explanation.

7. Dislocation particle velocities

Using the values for dislocations and rise times given in Tables 1 and 2 to compute dislocation particle velocities results in the conclusion that the logarithmically averaged velocity for a particle on the fault is 43 cm s^{-1} and in the regions of asperities this average is about 103 cm s^{-1} (assuming that the motion is symmetric with respect to the fault). These values are averages throughout the duration of the slip pulse, and the particle velocities may be considerably higher (perhaps 10–20 m s^{-1}) in the immediate vicinity of the rupture front.

These dislocation particle velocity estimates have disturbing engineering consequences for some classes of structures located very close to large earthquakes. For example, dislocations of 7 m were observed for some sections of the San Andreas fault during the 1906 San Francisco earthquake. This implies that some regions near the fault shifted their position with respect to an inertial frame by at least 3.5 m in several seconds. This may prove to be an engineering problem for some structures. In particular, base-isolated buildings are usually designed with the assumption that short-period (< 5 s) ground motions are less than 50 cm.

8. Conclusions

It has been demonstrated that slip durations for a given point on a fault (dislocation rise times) deduced from many rupture models derived from seismic waveform data are significantly shorter than the time required to notify points on the fault that the rupture has stopped. These slip durations are about 15% (or perhaps less) as long as the slip durations that result from dynamic crack-like rupture models. One explanation is that long-period parts of the fault slip history are unresolved from these models, which would imply that they have seriously underestimated the total slip for earthquakes. However, evidence has been presented

that the slip durations are indeed short. Several potential models result in short slip durations. In the first, earthquakes are composed of a sequence of small dimension (short duration) events that are separated by locked regions (barriers). However, in at least some of the dislocation models for specific earthquakes, it appears that the slip is relatively smoothly distributed (no barriers), and yet, the duration of slip is short. In the second model, rupture occurs in a narrow self-healing pulse of slip that travels along the fault surface. In this model, the frictional strength on the fault is high everywhere except in the immediate vicinity of the rupture pulse. It is suggested that the frictional strength of the fault is inversely related to the dislocation particle velocity in the slip pulse, perhaps caused by intense compressional waves that would tend to decrease confining stresses locally in the region of the slip pulse.

It is suggested that this dislocation-velocity-weakening, slip-pulse model may allow for the following features: the static strength of fault materials at seismogenic depths may be relatively high (on the order of kilobars); the ambient stress in the vicinity of active faults may be any value between several hundred bars and a kilobar (depending on the size and frequency of occurrence of the slip pulses that propagate on the fault); the frictional stress during slip may be less than several hundred bars (thereby generating relatively little heat); the average dynamic stress drop in the region of the slip pulse is on the order of 50–100 bars; the average static stress drop may be relatively low (tens of bars) and is controlled by the final length that a slip pulse will propagate; large-amplitude slip pulses tend to propagate long distances; regions that do not efficiently propagate slip pulses may accumulate high ambient stresses and may be regions that nucleate many small earthquakes; and regions that do support the propagation of large slip pulses maintain relatively lower ambient stresses and would rarely produce rupture nucleation. This model would tend to de-emphasize the importance of static stress drop in the region of large earthquakes and may help to explain why some earthquake recurrence times are surprisingly irregular.

Kinematic models of fault rupture in which slip occurs in a short time period after the passage of a rupture front (often referred to as dislocation models) have been very successful for matching waveforms over a broad range of frequencies. However, they have often been criticized on the basis that they violate basic physical constraints. In this paper, a mechanism has been suggested that would produce the types of slip pulses that seem to fit waveform data so well. While the hypothesized slip-pulse model presented here is admittedly speculative, it does seem to provide a solution for a first-order problem that any model of rupture must ultimately deal with. It is now clear that the ambient shear stress and dynamic friction on the San Andreas fault are low compared to the confining pressure at seismogenic depths. Realistic rupture models must satisfy this constraint.

Acknowledgements

Because of the speculative nature of this study, I sought the opinion of many of my colleagues. I particularly thank William Ellsworth who suggested several key ideas concerning the importance of rupture propagation, and Jim Brune who generously shared several key ideas about sliding friction. I also thank Jim Knowles, Jim Rice, Jim Dieterich, Hiroo Kanamori, Paul Okubo, Stephen Hartzell, Steven Day, and Tom Hanks who made valuable comments and who bear no responsibility if this model turns out to be incorrect. I thank Wayne Thatcher, Jack Boatwright, Jim Brune, Joe Andrews, Steve Wesnousky, Dave Boore, and an anonymous referee for their reviews of the manuscript. Finally, I thank Carlos Mendoza for providing the displacement time series for the Michoacan earthquake.

References

Aki, K., 1979. Characterization of barriers on an earthquake fault. J. Geophys. Res., 84: 6140–6148.

Aki, K. and Richards, P.G., 1980. Quantitative Seismology, Vol. II. W.H. Freeman and Company, San Francisco, 932 pp.

Anderson, J.G., Bodin, P., Brune, J.N., Prince, J., Singh, S.K.,

Quaas, R. and Onate, M., 1986. Strong ground motion from the Michoacan, Mexico, earthquake. Science, 233, 1043–1049.

Archuleta, R.J. and Frazier, G.A., 1978. Three-dimensional numerical simulation of dynamic faulting in a half-space. Bull. Seismol. Soc. Am., 68: 541–572.

Beroza, G.C. and Spudich, P., 1988. Linearized inversion for fault rupture behavior: application to the 1984 Morgan Hill, California, earthquake. J. Geophys. Res., 93: 6275–6296.

Bodin, P.A. and Brune, J.N., 1990. Scaling of displacement with rupture length for shallow earthquakes. Bull. Seismol. Soc. Am. (submitted).

Bouchon, M., 1982. The rupture mechanism of the Coyote Lake earthquake of 6 August 1979 inferred from near-field data. Bull. Seismol. Soc. Am., 72: 745–757.

Brune, J.N., 1970. Tectonic stress and spectra of seismic shear waves from earthquakes. J. Geophys. Res., 75: 4997–5009.

Brune, J.N., 1976. The physics of earthquake strong motion. In: C. Lomnitz and E. Rosenblueth (Editors), Seismic Risk and Engineering Decisions. Elsevier, New York, pp. 141–171.

Brune, J.N., 1979. Implications of earthquake triggering and rupture propagation for earthquake prediction based on premomitory phenomena. J. Geophys. Res., 84: 2195–2198.

Brune, J.N., Henyey, T.L. and Roy, R.F., 1969. Heat flow, stress, and rate of slip along the San Andreas fault, California. J. Geophys. Res., 74: 3821–3827.

Brune, J.N., Fletcher, J., Vernon, F., Haar, L., Hanks, T. and Berger, J., 1986. Low stress-drop earthquakes in the light of new data from the Anza, California, telemetered digital array. In: S. Das, J. Boatwright and C.H. Scholz (Editors), Earthquake Source Mechanics. Am. Geophys. Union, Washington, DC, Geophys. Monogr., 37: 237–245.

Brune, J.N., Johnson, P.A. and Sclater, C., 1989. Constitutive relations for foamrubber stickislip. Seism. Res. Lett., 60: 26.

Brune, J.N., Johnson, P.A. and Sclater, C., 1990. Nucleation, predictability, and rupture mechanism in foam rubber models of earthquakes. Rubey Symposium Vol., University of California, LA, submitted.

Burridge, R. and Knopoff, L., 1967. Model and theoretical seismicity. Bull. Seismol. Soc. Am., 57: 341–371.

Chen, Y.T., Chen, S.F. and Knopoff, L., 1987. Spontaneous growth and autonomous contraction of a two-dimensional earthquake fault. Tectonophysics, 144: 5–17.

Das, S., 1988. Relation between average slip and average stress drop for rectangular faults with multiple asperities. Bull. Seismol. Soc. Am., 78: 924–930.

Day, S., 1982. Three-dimensional finite-difference simulation of fault dynamics: rectangular faults with fixed rupture velocity. Bull. Seismol. Soc. Am., 72: 705–727.

Dieterich, J.H., 1979. Modeling of rock friction; 1. experimental results and constitutive equations. J. Geophys. Res., 84: 2161–2168.

Eshelby, J.D., 1957. The determination of the elastic field of an ellipsoidal inclusion and related problems. Proc. R. Soc. London Ser. A, 241: 376–396.

Frankel, A. and Wennerberg, L., 1989. Microearthquake spectra from the Anza, California, seismic network: site response and source scaling. Bull. Seismol. Soc. Am., 79: 581–609.

Freund, L.B., 1979. The mechanics of dynamic shear-crack propagation. J. Geophys. Res., 84: 2199–2209.

Hartzell, S.H., 1989. Comparison of seismic waveform inversion techniques for the rupture history of a finite fault: application to the 1986 North Palm Springs, California, earthquake. J. Geophys. Res., 94: 7515–7534.

Hartzell, S.H. and Heaton, T.H., 1983. Inversion of strong ground motion and teleseismic waveform data for the fault rupture history of the 1979 Imperial Valley, California, earthquake. Bull. Seismol. Soc. Am., 73: 1553–1583.

Hartzell, S.H. and Heaton, T.H., 1986. Rupture history of the 1984 Morgan Hill, California, earthquake from the inversion of strong motion records. Bull. Seismol. Soc. Am., 76: 649–674.

Haskell, N.A., 1964. Total energy and energy spectral density of elastic wave radiation from propagation faults. Bull. Seismol. Soc. Am., 54: 1811–1841.

Heaton, T.H., 1982. The 1971 San Fernando earthquake; a double event? Bull. Seismol. Soc. Am., 72: 2037–2062.

Heaton, T.H., 1985. A model for a seismic computerized alert network. Science, 228: 987–990.

Jeffreys, H., 1959. The Earth. Cambridge University Press, 165 pp.

Kagan, Y.Y. and Jackson, D.D., 1990. Seismic gap hypothesis: ten years after. J. Geophys. Res., submitted.

Kanamori, H. and Allen, C.R., 1986. Earthquake repeat times and average stress drop. In: S. Das, J. Boatwright and C.H. Scholz (Editors), Earthquake Source Mechanics. Am. Geophys. Union, Washington, DC, Geophys. Monogr., 37: 227–235.

Kanamori, H. and Anderson, D.L. 1975. Theoretical basis of some empirical relations in seismology, Bull. Seismol. Soc. Am., 65: 1073–1095.

Kostrov, B., 1966. Self-similar problems of propagation of shear cracks. J. Appl. Math. Mech., 28: 1077–1078.

Lachenbruch, A.H., 1980. Frictional heating, fluid pressure, and the resistance to fault motion. J. Geophys. Res., 85: 6097–6112.

Lachenbruch, A.H. and Sass, J.H., 1973. Thermo-mechanical aspects of the San Andreas fault system. In: A. Nur (Editor), Proc. Conf. Tectonic Problems of the San Andreas Fault System. Stanford University Press, Stanford, CA, pp. 192–205.

Lachenruch, A.H. and Sass, J.H., 1980. Heat flow and energetics of the San Andreas fault zone. J. Geophys. Res., 85: 6185–6222.

Liu, H.L. and Helmberger, D.V., 1983. The near-source ground motion of the 6 August 1979 Coyote Lake, California, earthquake. Bull. Seismol. Soc. Am., 73: 201–218.

Liu, H.L. and Helmberger, D.V., 1985. The 23:19 aftershock of the 15 October 1979 Imperial Valley earthquake: more evidence for an asperity. Bull. Seismol. Soc. Am., 75: 689–708.

McCann, W.R., Nishenko, S.P., Sykes, L.R. and Krause, J.,

1979. Seismic gaps and plate tectonics: seismic potential for major boundaries. PAGEOPH 117: 1082–1147.

Melosh, H.J., 1979. Acoustic fluidization: a new geologic process? J. Geophys. Res., 84: 7513–7520.

Mendoza, C. and Hartzell, S.H., 1988. Inversion for slip distribution using GDSN P waves: North Palm Springs, Borah peak, and Michoacan earthquakes. Bull. Seismol. Soc. Am., 78: 1092–1111.

Mendoza, C. and Hartzell, S.H., 1989. Slip distribution of the 19 September 1985 Michoacan, Mexico, earthquake: near-source and teleseismic constraints. Bull. Seismol. Soc. Am., 79: 655–669.

Nabarro, F.R.N., 1967. Theory of Cyrstal Dislocations. Dover Publications, Inc., New York, 821 pp.

Oden, J.T. and Martins, J.A.C., 1985. Models and computation methods for dynamic friction phenomena. Comp. Meth. Appl. Mech. Engng., 52: 527–534.

Okubo, P.G., 1989. Dynamic rupture modeling with laboratory-derived constituative relations. J. Geophys. Res., 94: 12 321–12 335.

Papageorgiou, A. and Aki, K., 1983a. A specific barrier model for the quantitative description of inhomogeneous faulting and the prediction of strong ground motion. I. Description of the model. Bull. Seismol. Soc. Am., 73: 693–722.

Papageorgiou, A. and Aki, K., 1983b. A specific barrier model for the quantitative description of inhomogeneous faulting and the prediction of the strong ground motion. II. Applications of the model. Bull. Seismol. Soc. Am., 73: 953–978.

Parsons, I.D., Hall, J.F. and Lyzenga, G.A., 1988. Relationships between the average offset and the stress drop for two- and three-dimensional faults. Bull. Seismol. Soc. Am., 78: 931–945.

Pelton, J.R., Meissner, C.W. and Smith, K.D., 1984. Eyewitness account of normal surface faulting. Bull. Seismol. Soc. Am., 74: 1083–1089.

Rice, J.R. and Tse, S.T., 1986. Dynamic motion on a single degree of freedom system following a rate- and state-dependent friction law. J. Geophys. Res., 91: 521–530.

Richards, P.G., 1976. Dynamic motions near an earthquake fault: a three-dimensional solution. Bull. Seismol. Soc. Am., 66: 1–32.

Ruppert, S.D. and Yomogida, K., 1990. A crack-like rupture model for the 19 September 1985 Michoacan, Mexico, earthquake. Bull. Seismol. Soc. Am., submitted.

Salyards, S.L., 1989. Dating and Characterizing Late Holocene Earthquakes using Paleomagnetics, Ch. 5, Ph. D. Thesis, California Institute of Technology, Pasadena, 217 pp.

Scholz, C.H., 1982. Scaling laws for large earthquakes: consequences for physical models. Bull. Seismol. Soc. Am., 72: 1–14.

Shimazaki, K. and Nakata, T., 1980. Time-predictable recurrence model for large earthquakes. Geophys. Res. Lett., 1: 279–282.

Sibson, R.H., 1973. Interactions between temperature and pore fluid pressure during faulting and a mechanism for partial or total stress relief. Nature, 243; 66–68.

Tolstoi, D.M., 1967. Significance of the normal degree of freedom and natural normal vibrations in contact friction. Wear, 10; 199–213.

Tucker, B.E. and Brune, J.N., 1977. Source mechanism and m_b–M_s analysis of aftershocks of the San Fernando earthquake. Geophys. J. R. Astron. Soc., 49: 371–426.

Wallace, R.E., 1984. Eyewitness account of surface faulting during the earthquake of 28 October 1983 Borah Peak, Idaho. Bull. Seismol. Soc. Am., 74: 1091–1094.

Yoffe, E.H., 1951. The moving Giffith crack. Phil. Mag., 42; 739–750.

Zoback, M.D., Zoback, M.L., Mount, V.S., Suppe, J., Eaton, J.P., Healy, J.H., Oppenheimer, D., Reasenberg, P., Jones, L., Raleigh, B., Wong, I.G., Scotti, O. and Wentworth, C., 1987. New Evidence on the state of stress of the San Andreas fault system. Science, 238: 1105–1111.